Heat transfer characteristic modelling and the effect of operating conditions on re-cooled cycle for a scramjet

W. Bao, J. Qin and W. X. Zhou
Harbin Institute of Technology
Heilongjiang,
China

ABSTRACT

A re-cooled cycle has been proposed for a regeneratively cooled scramjet to reduce the hydrogen fuel flow for cooling. Upon the completion of the first cooling, fuel can be used for secondary cooling by transferring the enthalpy from fuel to work. Fuel heat sink (cooling capacity) is thus repeatedly used and fuel heat sink is indirectly increased. Instead of carrying excess fuel for cooling or seeking for any new coolant, the cooling fuel flow is reduced, and fuel onboard is adequate to satisfy the cooling requirement for the whole hypersonic vehicle. A performance model considering flow and heat transfer is build. A model sensitivity study of inlet temperature and pressure reveals that, for given exterior heating condition and cooling panel size, fuel heat sink can be obviously increased at moderate inlet temperature and pressure. Simultaneously the low-temperature heat transfer deterioration and Mach number constrains can also be avoided.

NOMENCLATURE

A	heat transfer surface area
a	sonic speed
C_p	specific heat of fuel
D	equivalent diameter
ff	friction factor
h	heat transfer coefficient
H	channel height
L	length
M	Mach number
m	mass flow rate of fuel
Nu	Nusselt number
P	pressure
ΔP	pressure drop
Pr	Prandtl number
Q	heat transfer rate
q_w	heat flux
Re	Reynolds number
s	heated wall thickness
T	temperature
t	the fin thickness
u	velocity
W	channel width
w	specific power
x	distance from entrance of cooling panel
δ	multiplication ratio of fuel heat sink
λ	thermal conductivity
η	efficiency
γ	adiabatic index
π	expansion pressure ratio
ρ	density

Paper No. 3438. Manuscript received 31 May 2009, revised version received 22 November 2009, 2nd revised version received, 6 June 2010, accepted 30 September 2010.

https://doi.org/10.1017/S0001924000005479 Published online by Cambridge University Press

Subscripts

a	property evaluated at average temperature of coolant reference
b	property evaluated at bulk temperature reference
c	coolant
C	cooling channel
f	fin
i	inlet
j	segment number along the length of cooling channel
lim	limit value
net	net available work
o	outlet
P	panel
p	pump
r	regenerative cooling
t	turbine
wc	coolant side wall
wg	gas side wall
1	first cooling
2	second cooling

1.0 INTRODUCTION

Hypersonic airbreathing vehicles are an attractive technology for air launched strike weapons, aerospace planes, fully reusable space transport vehicles, due to their long range, rapid response time and high impact velocity. Hypersonic vehicles are also the most likely and useful near-term application of supersonic combustion ramjet (scramjet) propulsion systems[1,2,3]. One of the key issues of hypersonic flight is the thermal protection of the overall vehicle and more specifically the cooling of the scramjet engine, since even composite materials can not withstand the large heat load found in a scramjet combustion chamber. Regenerative cooling with fuel used as the coolant is generally regarded as the only feasible solution[4]. In this way, fuel flows through the cooling passage to cool the engine walls before it is used for combustion[5]. However, limited fuel onboard and corresponding limited fuel heat sink can barely meet the cooling requirements for the whole vehicle. According to the previous studies on hydrogen fuelled scramjets, coolant flow rates exceed the stoichiometric flow rates in the high flight Mach number region beyond Mach 10[6]. This means the fuel heat sink is insufficient, for instance, the maximum fuel flow rate for cooling is two times bigger than that for propulsion in the joint CIAM-NASA Mach 6·5 scramjet flight programme[7]. And so, more fuel than required for propulsion must be carried for the mission and the excess fuel has to be abandoned[8]. Additional hardware and extra fuel will increase the size, weight and complexity of the vehicle, which, in return, will significantly degrade its performance. It is therefore very important to increase the fuel heat sink for a high speed scramjet.

Developing endothermic fuels is a very effective method for increasing hydrocarbon fuel chemical heat sink[9]. However, the coking potential of a hydrocarbon at high temperatures limits the hydrocarbon fueled scramjet engine to approximately Mach 8[10]. Since coking within the cooling channels must be avoided at all costs, temperature is controlled to be below the coking temperature. And it is generally accepted that hydrogen can not perform endothermic conversion. It was also suggested that the heat sink of hydrogen fuel will not be increased even when excess hot fuel re-enters the tank. In addition, vaporised fuel will take up a considerably larger volume than liquid. So a limit is imposed on the amount of heat storable in this manner without larger tankage[11]. So far, no method can be used to directly increase the heat sink of hydrogen fuel.

A re-cooled cycle was recently advanced, which is an indirect method to increase fuel heat sink by multiple repeatedly utilising fuel heat sink. Previous thermodynamic cycle analysis show that re-cooled cycle (RCC) could remarkably increase fuel heat sink without introducing new component or weight penalty[12,13]. An analytical fin-type model for incompressible flow in smooth-wall rectangular ducts in terms of hydrodynamic, thermal, power balance and Mach number constraints is proposed. The prime objective of this article is to discuss the effect of inlet temperature and pressure these two operating condition parameters of the cycle on the performance of re-cooled cycle.

2.0 NOTIONAL SCHEMATIC AND OPERATING PRINCIPLE OF RCC

A conceptual, two-dimensional scramjet engine cross section is shown in the bottom of Fig. 1. The engine consist of a series of ramps that merge with the vehicle lower surface, and a cowl which helps capture the air compressed by the vehicle fuselage and the engine ramps. The major components of the engine are the inlet, combustor, and nozzle.

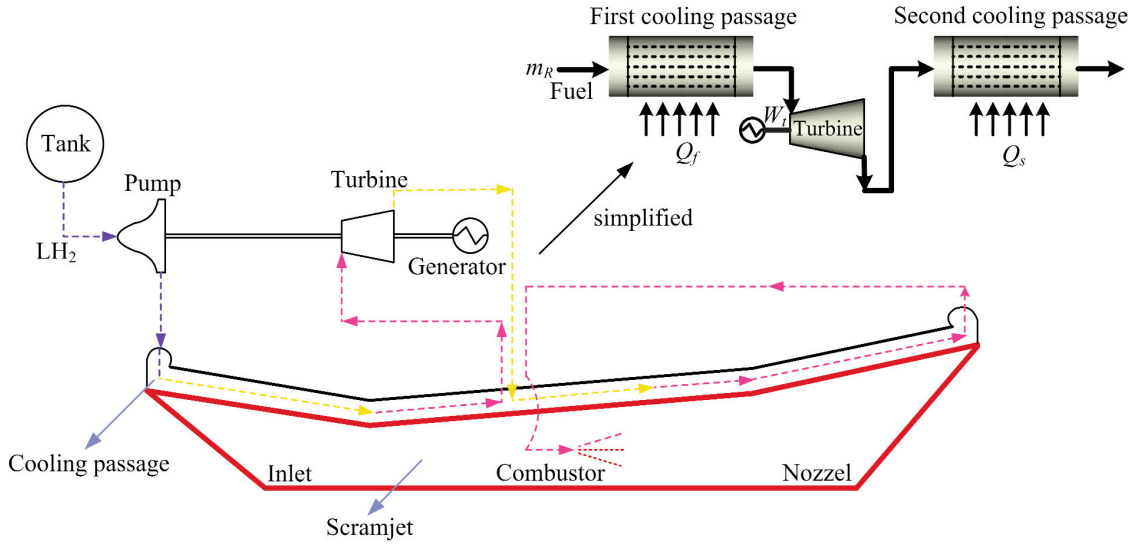

Figure 1 Generic configuration of a scramjet engine with re-cooled cycle.

https://doi.org/10.1017/S0001924000005479 Published online by Cambridge University Press

Re-cooled cycle (RCC) has been put forwarded[14]. As shown in Fig. 1, RCC is mainly composed of the first and second cooling passages, a pump, and a turbine. Unlike a traditional turbine, the primary purpose of the turbine is designed to decrease fuel temperature instead of doing work. Dashed lines in Fig. 1 show the flow process of fuel. First, the fuel coming out from the fuel tank is pumped to the supercritical pressure, and then enters into the first cooling passage to cool the heated surfaces, and its temperature reaches its maximum value; second, the high temperature and high pressure fuel expands while doing work to the turbine, and its temperature decreases; third, fuel enters the second cooling passage to perform secondary cooling; before it enters into the combustion chamber.

Compared to traditional regenerative cooling, additional heat could be absorbed for per unit of fuel through secondary cooling in RCC, fuel heat sink could be regarded as an indirect improvement. And this will effectively reduce fuel flow rate for cooling in terms of the overall cooling requirement of the vehicle. In addition, the work output of the turbine can drive the fuel pump and an electric generator to provide the power for vehicle subsystems, such as radar communication system, flight control system, electronic equipment, and environmental control system, and so forth. The fuel pump and turbine in RCC perform the same function as the turbo-pump fuel feeding system of scramjet. Therefore, RCC could also be regarded as a thermodynamic power system, which can partially replace the original power supply system. In summary, a RCC system is compatible with other subsystems in terms of interconnection and function.

The RCC uses the available energy of fuel itself to drive the cycle, combines functions of existing scramjet components, and uses the sectional design characteristics of cooling passage. No new component or weight penalty is introduced. Furthermore, RCC is simple and easy to be executed compared to other methods to increase the fuel heat sink. Once RCC is applied, it maybe unnecessary to take excessive fuel for cooling or seek for any new coolant.

3.0 ANALYTICAL MODEL AND METHODOLOGY

Cooling channel, turbine and pump are the key components in RCC, a model of RCC consisting of components performance, flow and heat transfer in them is considered, as well as thermal, hydrodynamic, Mach number and power balance limitations.

3.1 Channel geometry and basic assumptions

The present work considers a single cooling panel shown in Fig. 2, which is composed by many rectangular duct geometry cooling channels[15]. For convenient analysis, the panel is divided into segments along the flow length. The panel has a length (L_p) of 1m, a width (W_p) of 1m. And the thickness of the heated wall (s) is 1mm and the rib thickness (t) is 0·2mm.

The heated wall is exposed to an uniform q_w, the lower surface (the inner wall) is assumed to be an adiabatic boundary since the amount of heat transferred through the inner wall is small compared to the heat going into the coolant. Coolant flow and heat flux are assumed to be uniform across the width of the panel, and thus the coolant and structural temperatures do not vary across the panel width. So the constant area, constant heat flux, rectangular duct geometry, single cooling channel is chosen as the study object and shown in Fig. 3. The channel has a channel width (W) of 2mm and a channel height (H) of 2mm, so the equivalent diameter (D) is 2mm and a flow area is 4mm^2. For RCC, the cooling channel is divided into two sections with fixed total length L_p.

The basic analysis approach employed was to assume a steady state quasi one-dimensional energy balance across the regenerative

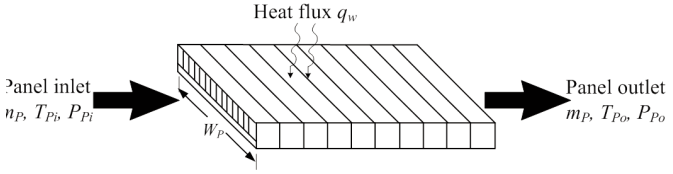

Figure 2 Cooling jacket flow and thermal models.

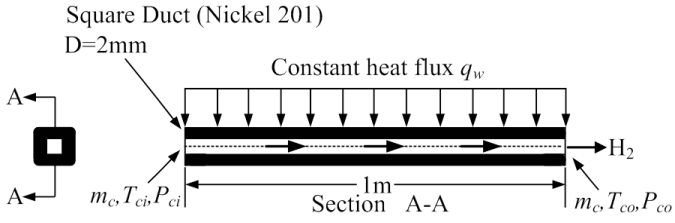

Figure 3. Single cooling channel schematic.

cooling jacket. First, an analytical model based on fin-type assumptions and existing correlations for heat transfer for smooth walls is introduced. To further simplify the analysis, an analytical model will be developed under the following assumptions:

1. All energy transferred across the coolant wall is absorbed by the coolant.
2. There exists no temperature variation in the cross section of the duct walls (fin assumption).
3. The channel walls are assumed to be smooth.
4. Wall-conduction in axial direction is negligible.
5. The flow is fully developed.
6. All data sets are screened to rule out buoyancy effects.
7. All the thermalphysical properties except density are regarded as constant for different pressure, they only vary considerably with temperature.

Property values for hydrogen are obtained from the National Institute of Standards and Technology (NIST) Thermodynamic and Transport Properties of Pure Fluids database and the NIST Chemistry WebBook[16]. The specific property variations that must be considered are specific heat, thermal conductivity, density and viscosity.

The coolant flow conditions, as well as each of the design requirements, are evaluated at the exit of each segment. A brief description of the various analytical models which describe the actively cooled channel performance follows.

3.2 Thermal and flow analysis in cooling channel

Figure 4 illustrates the division of the cooling panel into segments with length L for purposes of the analysis. A representative segment with entrance temperature T_j and pressure P_j is shown in the lower portion of Fig. 2. It is subjected to heat flux q_w. The analysis scheme marches through the cooling channel, beginning where the coolant enters the jacket and continues until the coolant exits the channel. At each discrete axial location, dx, a control volume analysis is performed. The general equation describing the energy balance is given in Equation (1):

$$Q_j = mC_{pj}(T_{j,o} - T_{j,i}) = h_j(T_{j,a})A_c + q_{j,f}A_f \quad \ldots (1)$$

https://doi.org/10.1017/S0001924000005479 Published online by Cambridge University Press

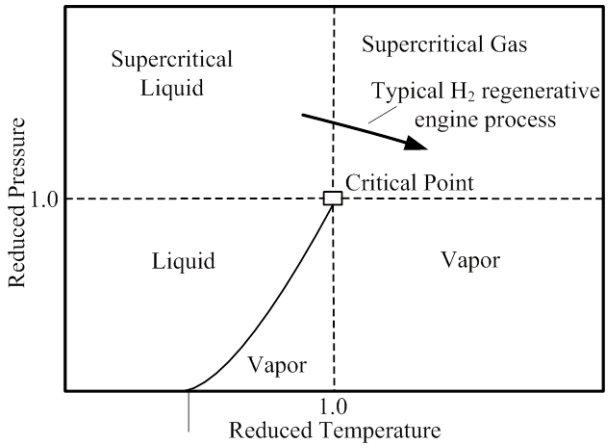

Figure 4. Typical H_2 regenerative cooling conditions with hydrogen as coolant.

Where $A_C = WL$ is the non-finned convecting surface area and A_f is the convecting surface area of the fin or rib, as shown in Fig. 5. And the properties are evaluated at the average temperature of segment inlet and outlet temperature of coolant.

As shown in Fig. 3 that the rib surface provides additional wetted coolant surface area providing a fin effect for the cooling channel. To calculate the additional heat transfer from the finned surface area, a fin efficiency is calculated as outlined assuming an adiabatic tip as[17]:

$$\eta_f = \frac{th(eH_f)}{eH_f} \quad \ldots (2)$$

Where, $Hf = H + t/2$. And e as an intermediate parameter is defined by Equation (3):

$$e = \sqrt{\frac{2h}{\lambda t}} \quad \ldots (3)$$

From the fin efficiency, a corresponding heat flux is calculated for the fin as:

$$q_{j,f} = h_j(T_{j,wc} - T_{j,a})\eta_f \quad \ldots (4)$$

And the outlet temperature of segment j is the entrance temperature of segment $j + 1$, as well other flow parameters of hydrogen. As the heat balance calculation is performed one segment after another, the outlet temperature of two sections of cooling passages will be eventually obtained. Once the coolant conditions at the exit of a segment are determined, the temperature distribution through the cooling channel at the segment exit (the hottest location in a segment) is evaluated.

The next step is to compute the film coefficient for convective heat transfer using published correlations. Turbulent Nusselt number correlation developed by M.F. Taylor[18] is chosen to determine the heat transfer coefficient for the channel-fin cooling channel. This equation uses the surface to bulk temperature ratio and also considers the entrance effects. And this correlation for turbulent flows of hydrogen in tubes is correlated over a wide range of temperatures, pressure and heat fluxes. The correlation is:

$$Nu = 0{\cdot}023Re^{0{\cdot}8}Pr^{0{\cdot}4}(T_{wc}/T_b)^{-(0{\cdot}57\text{-}1{\cdot}59D/x)} \quad \ldots (5)$$

Where we choose $T_{j,i}$ as T_b to evaluate fuel property. The difference between gas side wall temperature T_{wg} and coolant side wall temperature T_{wc} can be obtained by wall conduction equation as:

$$q_j = \frac{\lambda}{s}(T_{wg} - T_{wc}) \quad \ldots (6)$$

The coolant pressure drop across a segment can be estimated by the Darcy-Weisbach equation[19],

$$\Delta P_j = ff\frac{\rho L u^2}{2D} \quad \ldots (7)$$

Where the friction factor ff is obtained from the Moody chart. For a smooth tube Reynolds number of 10,000, the Moody chart, ff is approximately 0·031[20].

3.3 Model for turbine and pump

The expander cycle used in a liquid rocket is also adopted as one potential scheme of fuel feeding cycle for a scramjet, so the pump and turbine are not new components for RCC. For the pump, the flow rate of the turbine is the same with that of the pump, so we are only concerned with the specific power, which can be estimated as[21]:

$$w_p = \frac{P_{po} - P_{pi}}{\eta_p \rho_{pi}} \quad \ldots (8)$$

The fuel/coolant is hydrogen stored cryogenically as a liquid at 20K and 240kPa. In typical scramjet applications, hydrogen enters the cooling passages as a liquid above the critical pressure (P_{cr} = 1·3 MPa) and at temperatures as low as 25K, which is well below the critical temperature (T_{cr} = 33K). As the hydrogen continuously flows through the channels, it is quickly heated to above the critical temperature, where it becomes a supercritical gas (see Fig. 6)[22]. The value of fuel pressure varies within 2~20MPa in Ref. 15.

Under the assumptions that there is no loss of power because of friction of the mechanical systems, the turbine exit temperature can be calculated as[23]:

$$T_{to} = T_{ti}\left\{1 - \eta_t\left[1 - \pi^{(1-K)/K}\right]\right\} \quad \ldots (9)$$

Specific power rate of turbine is calculated by the following equation[21]:

$$w_t = \eta_t C_P T_{ti}[1 - \pi^{(1-K)/K}] \quad \ldots (10)$$

Efficiencies of the pump and the turbine in Equations (8) and (10) are estimated on the basis of typical values for turbopumps of rocket engines, because the operating condition of scramjet turbopumps will be similar to that of rocket engine turbopumps. Efficiency of the hydrogen pump is 70%, and the turbine of the EC is assumed to be a reaction turbine with efficiency of 80%[21].

3.4 Material properties and code validation

High conductivity materials are generally used in the cooling channel construction. Nickel 201 is chosen as the material used in the studies, which offers a range of the important material properties such as thermal conductivity, high temperature capability, and strength. Nickel 201 offers moderate thermal conductivity λ (60·6W/m.K) and higher temperature capability (1,110K) compared with other alloys. These properties along with high ductility for fatigue resistance make nickel an attractive choice for a cooling channel[24].

Material thermal conductivities are included as functions of the average cooling-channel temperature in the one-dimensional model. Detailed two- and three-dimensional finite element models verified the accuracy of temperatures computed from the simple models to be within ten percent over a wide range of geometries, convective film coefficients, and thermal conductivities. The accuracy of the simple

https://doi.org/10.1017/S0001924000005479 Published online by Cambridge University Press

one-dimensional model for hydrogen convective cooling had also been verified by many other researchers[22,25].

3.5 Limitation consideration

The active cooling thermal analysis of RCC must also satisfy the requirements such as material limits on cooling-channel temperature, limits on coolant Mach number, the outlet pressure limit, stress, and as well as fatigue life. Also the power balance between turbine and pump, which is a new limit not need to consider in conventional regenerative cooling. In this paper, we only consider the former three limitations and the power balance limit.

To avoid compressibility effects, a limit is needed for the Mach number of the coolant flow. The Mach number is calculated by

$$M = \frac{m}{\rho a W H} \quad \ldots (11)$$

Where all the coolant conditions are evaluated at the channel outlet. The estimated speed of sound for hydrogen fuel is about 1,000ms^{-1}, and a Mach number limit M_{lim} = 0·25 was used by Scotti *et al*[26]. This condition can be satisfied simply by limiting u less than 250ms^{-1}, and no constraint function is required.

For material limits on cooling channel temperature, the cooling channel wall temperature should be maintained under the material limit, we set T_{lim} = 1,110K.

The outlet pressure limit of the hydrogen should be maintained above a limit value for proper fuel flow and penetration into the airstream in the scramjet engine (hydrodynamic constraint). The pressure in the combustion chamber of scramjet is generally as low as 0·3MPa[27], considering the pressure loss from cooling passage outlet to combustor, we thus set P_{lim} = 0·6MPa.

Table 1 summarises the constraint functions needed to consider in the RCC thermal analysis procedure. The Mach-number and pressure constraint functions in Table 1 are evaluated at the channel exit[28].

Table 1
Constraint function in the thermal analysis

Constraints	Channel Temperature	$T_{wc} < T_{lim}$
	Outlet Pressure	$P_{co} > P_{lim}$
	Mach Number	$M < M_{lim}$
	Power Balance	$w_t > w_p$

3.6 Performance parameters

The objective of RCC is to reduce the fuel flow for cooling, which can be interpreted to increase the heat absorption by per unit of fuel. This is different from the conventional power cycle[29,30], and it is unsuitable to use thermal efficiency to evaluate the performance of RCC[31,32]. Thus, it is necessary to define several new performance parameters to compare the performance of RCC with that of regenerative cooling.

The prime function of RCC is to increase fuel heat sink. And the multiplication ratio of fuel heat sink intending to evaluate the performance of RCC has been defined[33] to demonstrate the extent of increasing the fuel heat sink, which is defined as:

$$\delta = \frac{Q_2}{Q_1} \quad \ldots (12)$$

Another performance gain of RCC is specific net work output w_{net}[34], which is the difference between specific power produced by turbine wt and power required by pump w_p

$$w_{net} = w_t - w_p \quad \ldots (13)$$

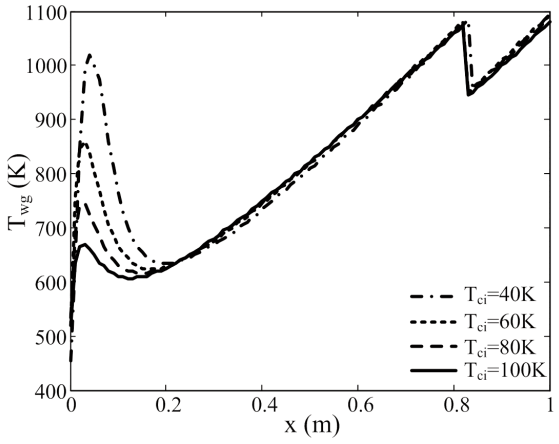

Figure 5. Variation of T_{wg} at different T_{ci} down the length of the channel.

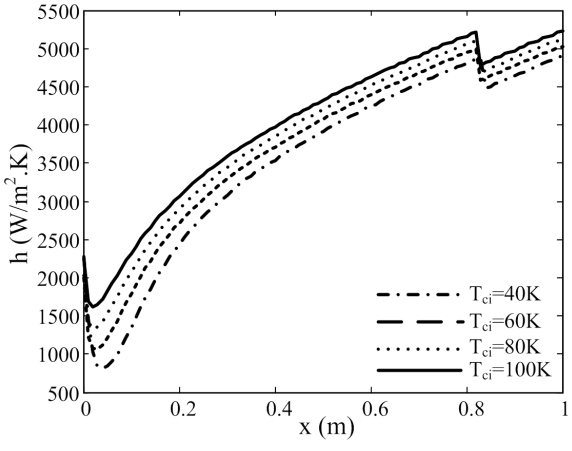

Figure 6. Variation of h at different T_{ci} down the length of the channel.

4.0 RESULTS AND DISCUSSION

Sensitivity analysis is an useful basis for system performance analysis and optimal design in order to find the effect law of each parameter and major factors. To examine the flow and heat transfer down the length of the cooling channel, to see how the cycle parameters influence the multiplication ratio of fuel heat sink (δ), as well as to illustrate potential performance of RCC, detailed numerical examples are provided. For given cooling channel structures, fixed T_{clim} and outlet pressure limit, inlet conditions (inlet temperature and pressure of fuel) are chosen here as the instance to analyse the effect of flow and component parameters on the performance of RCC and the flow and heat transfer down the length of channel.

4.1 Effect of inlet-temperature T_{ci}

Fig. 5 shows the variation of T_{wg} as a function of T_{ci} down the length of the channel, when P_{ci} = 4MPa, T_{clim} = 850K, γ = 1·4, and π = 2 and qw = 2MW/m^2, other parameters and conditions have been given in the analysis above. The results for T_{ci} = 40, 60, 80, 100K nearly fall on one curve at the latter half part (after x is bigger than 0·2m), which implies that the inlet temperature of fuel T_{ci} does not have any influence on T_{wg} for this part. However, T_{wg} varies greatly with T_{ci} in

https://doi.org/10.1017/S0001924000005479 Published online by Cambridge University Press

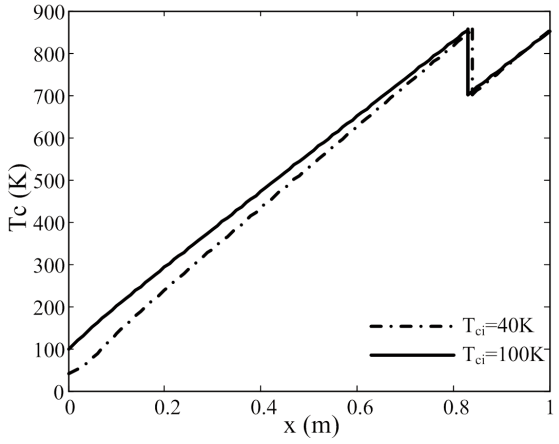

Figure 7. Variation of T_c at different T_{ci} down the length of the channel.

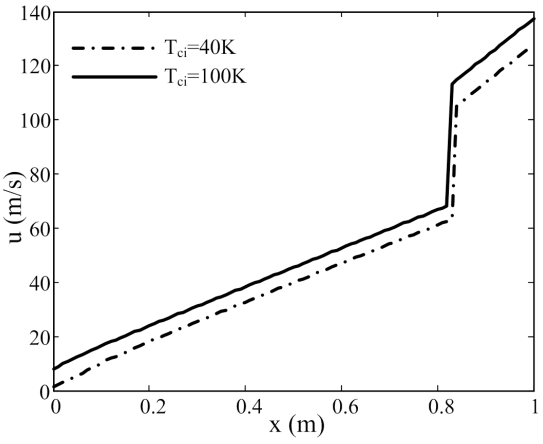

Figure 8. Variation of u at different T_{ci} down the length of the channel.

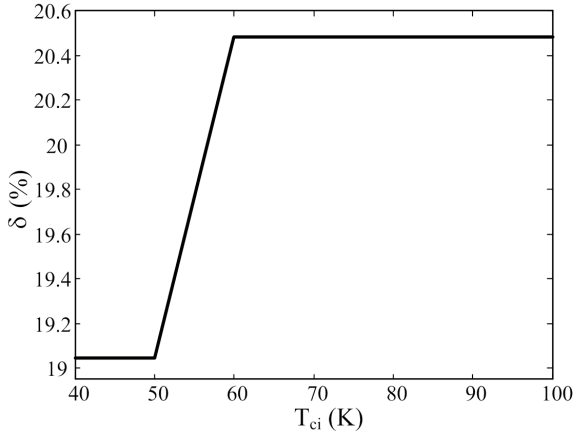

Figure 9. Variation of δ as T_{ci}.

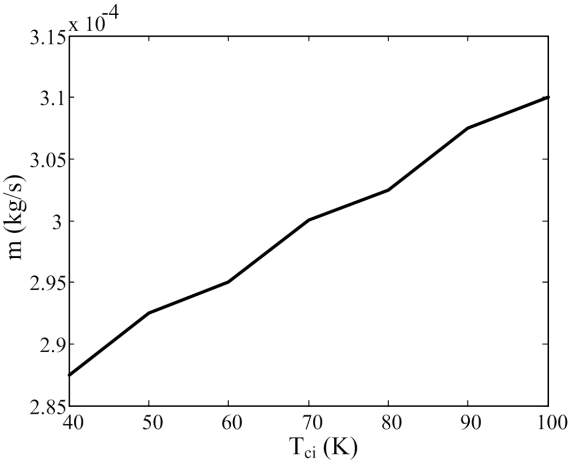

Figure 10. Variation of m as T_{ci}.

the entrance region of the cooling channel, and increases as the decrease of T_{ci}. Furthermore, there exits a temperature spike in the entrance region, the maximum value of T_{wg} in the entrance region is larger than 1,000K, which is close to the temperature limit of the wall. This phenomenon is called as 'heat transfer deterioration at low temperature', which has been reported by several researchers[35] and could be further illustrated by the variation of heat transfer coefficient h_c down the length of the cooling channel.

It can be seen from Fig. 6 that heat transfer coefficient has a sudden reduction in the entrance region, and hc gets its minimum value where T_{wg} gets its maximum value. The reason why the heat transfer deterioration occurs in the entrance region though the coolant is at lower temperature, it is because that the viscidity of hydrogen fuel firstly decreases and then increases with the increase of temperature. The heat transfer deterioration will make the heat transfer coefficient of cooling channel decrease, and will lead to over temperature for the wall. Therefore, the heat transfer deterioration has to be avoided. In practical applications, fuel must be preheated before entering the cooling channel, a possible way is that fuel is firstly usually used as the coolant for heat structure with lower heat load, such as cabin environment and the avionics, etc.

The variation of T_{wg} down the length of cooling channel is composed by two curves in Fig. 5 at each T_{ci}, there is a sudden decrease from the end of the first curve to the start of the second curve, and this variation can also be seen in Figs 6 and 7. Furthermore, the abscissa length of the first curve in each figure at every T_{ci} means the length of the first cooling passage L_1, and there is slight difference among the values of L_1 at different T_{ci}.

The sudden reduction of h at the entrance of the second cooling passage in Fig. 6 dose not lead to the sudden increase of T_{wg} in Fig. 5, because the fuel temperature T_c decreases greatly as shown in Fig. 7, and so the heat balance is still met. This is the desired results for the introduction of RCC, and can also be translated to that RCC will not bring with any disadvantage for the heat transfer process in some extend.

As shown in Fig. 7, the major difference of T_c between T_{ci} = 40K and T_{ci} = 100K occurs at the entrance, and the difference becomes more and more little down the length of the cooling channel, because m increases as T_{ci} for fixed outlet temperatures of the two cooling passages. Furthermore, T_c decreases greatly after expanding in the turbine, just the decrease of T_c brings with the variation of fuel property, the secondary cooling, the additional cooling capacity for per unit of fuel and other changes different with regenerative cooling. The temperature difference between the inlet and exit of turbine is about 150K, which would correspondingly increase when bigger π were adopted.

As shown in Fig. 8, the velocity of hydrogen fuel accelerates from a value of $8ms^{-1}$ at the first cooling passage entrance to a peak velocity value at the second cooling passage exit of $137{\cdot}3ms^{-1}$ when T_{ci} = 100K, which is nearly 17 times bigger than that of the inlet velocity. This just because the variable properties have a great effect on the velocity. Furthermore, the velocity at the entrance of the second cooling passage is about double that of the exit of the first cooling passage due to the severe change in density, for the pressure at the turbine outlet is two times that of the turbine inlet. Decrease of the fuel pressure at constant temperature implies a density decrease,

https://doi.org/10.1017/S0001924000005479 Published online by Cambridge University Press

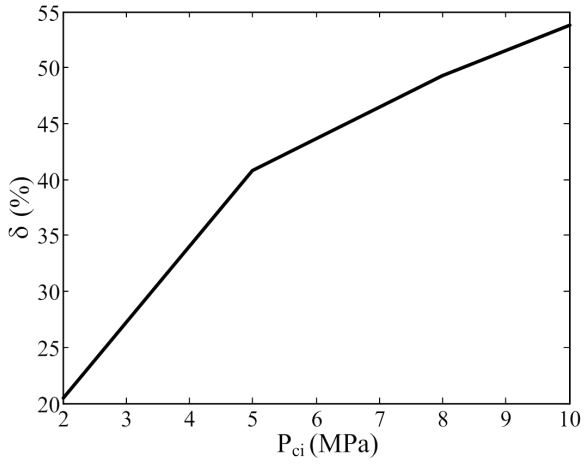

Figure 11. Variation of δ as P_{ci}.

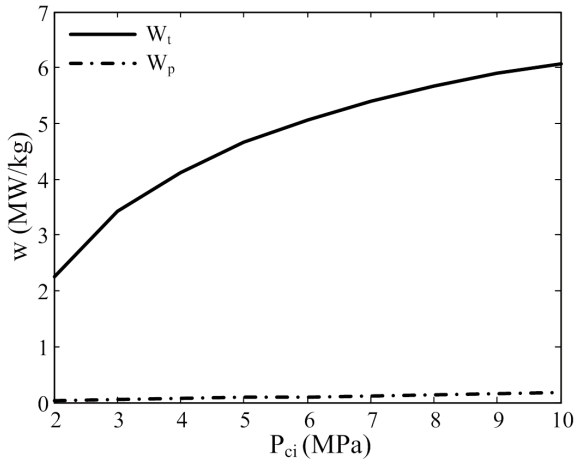

Figure 12. Variation of w_p and w_t as P_{ci}.

so the velocity of fuel must increase for fixed mass flow rate and constant flow area from. If bigger π were adopted, hydrogen fuel would accelerate to much higher velocity and the Mach number constrain may be activated.

As shown in Figs 9 that δ increases as T_{ci}, because the available temperature rise decreases as the increase of T_{ci} and the heat absorption Q_1 in the first cooling passage will correspondingly decrease. However, the heat absorption Q_2 in the second cooling passage keep a constant value at different T_{ci} due to fixed temperature rise for per unit of fuel. It can also be seen in Fig. 10 that fuel flow for cooling will increase as T_{ci}, for available cooling capacity decreases as the increase of T_{ci} in the first cooling passage for per unit of fuel, with fixed external heating.

Combining the results in Figs 9 and 10, δ and m both increase as T_{ci}, which may be seen as an opposite conclusion with the introduction of RCC at a first glance. However, the definition of δ should be at the premise of fixed fuel heat sink, but fuel heat sink decreases as T_{ci} increases. Therefore, if the variation of fuel heat sink were considered, the results in Fig. 9 could be easily understanded. In summary, the conclusion in Figs 9 and 10 are not inconsistent, and RCC is still helpful to reduce fuel flow for cooling. Furthermore, the effect of T_{ci} on m should be dealt as the convincing conclusion for the performance of RCC. T_{ci} should thus be chosen as small as possible to obtain lower m. However, we have concluded that bigger T_{ci} is helpful to avoid heat transfer deterioration. Synthetically, T_{ci} = 60K is a moderate value to avoid heat transfer deterioration and to reduce fuel flow for cooling.

4.2 Effect of inlet-pressure P_{ci}

It is found from analysis above that bigger ΔT_t (difference between inlet temperature and outlet temperature of the turbine) is advantageous to obtain higher δ, because heat absorption of fuel in the second cooling passage increases as ΔT_t. Furthermore, by Equation (9), ΔT_t is decided by T_{co}, η_t, γ and π. γ and η_t are regarded as the constant, and T_{co} = 850K is already at a high level in order to avoid over temperature phenomenon for the wall. Therefore, the major method to increase ΔT_t is to choose bigger π. And π is determined by P_{ci} and P_{co} without pressure loss. Taking into account of the outlet pressure limit, P_{ci} is chosen as the variable to examine the effect of P_{ci} or π on RCC and P_{co} is set nearly to be around 1MPa, i.e. P_{co} could not be maintain as a constant value due to the pressure loss. In the following, P_{ci} is set varying from 2MPa to 10MPa, and π varies correspondingly from 2 to 10. And T_{ci} = 60K, other parameters are the same with that in above calculation.

As shown in Fig. 11, δ increases as P_{ci} increases, which means that big P_{ci} or π is useful to increase fuel heat sink, i.e. to reduce fuel flow for cooling, and the variation of δ at different P_{ci} further illustrates this. But the slope of δ with P_{ci} is getting smaller as P_{ci} is bigger than 5MPa, which is only half of that when P_{ci} is smaller than 5MPa. This illustrates that the effect of P_{ci} on δ is weakening as the increase of P_{ci}. In summary, P_{ci} = 5MPa may be a moderate value with relatively high δ and good heat transfer effect without activating Mach number constrain.

As shown in Fig. 12, the value of w_t is about an order of magnitude higher than that of w_p for each P_{ci}, because the inlet temperature of the turbine is high and C_p of hydrogen is with a large value. Therefore, the power balance constrain will not be activated for almost any conditions. As an output of several MW/kg work can be utilised as the power source for the fuel feeding subsystem and power supply subsystem, to realise the full utilisation of energy for the entire hypersonic vehicle.

No doubt that we desire that δ can obtain a value as high as possible. However, we also have to consider the limitation constrains, heat transfer efficiency and practical operation condition of scramjet. If the introduction of RCC could make sure that the coolant flow rate equals to fuel flow rate, this result were just enough, and higher capacity of saving coolant flow rate may not be needed any more. So the practical operation of RCC needs to control the coolant flow rate at different conditions, and optimal design for RCC at off-design conditions is also important.

5.0 CONCLUSION

Influence of entrance parameters (inlet temperature and pressure) on the performance of RCC is discussed. The computational results show that the multiplication ratio of fuel heat sink can be as high as 53·85% and the minimum value of it is 19·05%. A model sensitivity study of inlet temperature and pressure these two entrance parameters reveals that, for given exterior heating condition and cooling panel size, fuel heat sink can be obviously increased at moderate inlet temperature and pressure, simultaneously, low-temperature heat transfer deterioration and over-velocity can also be avoided. For other given conditions, the optimal value of inlet temperature and inlet pressure may vary, but the calculation method is the same, and the effect law of inlet temperature and inlet pressure on cycle performance does not change.

ACKNOWLEDGMENTS

This work is supported by the National Natural Science Foundation of China (Grant No 51076035).

https://doi.org/10.1017/S0001924000005479 Published online by Cambridge University Press

REFERENCES

1. CHANG, J., BAO, W. and YU, D. Hypersonic inlet control with pulse periodic energy addition, *Proc IMechE Part G: J Aerospace Engineering*, 2009, **223**, (2), pp 85-94.
2. MAHAPATRA, D. and JAGADEESH, G. Shock tunnel studies on cowl/ramp shock interactions in a generic scramjet inlet, *Proc IMechE Part G: J Aerospace Engineering*, 2008, **222**, (8), pp 1183-1191.
3. KONTIS, K. Flow control effectiveness of jets, strakes, and flares at hypersonic speeds, *Proc. IMechE Part G: J Aerospace Engineering*, 2008, **222**, (5), pp 585-603.
4. GASCOIN, N., GILLARD, P., DUFOUR, E. and TOURE, Y. Validation of transient cooling modelling for hypersonic application, *J Thermophysics and Heat Transfer*, 2007, **21**, (1), pp 86-94.
5. CHANG, J. and BAO, W. Effects of wall cooling on performance parameters of hypersonic inlets, *Acta Astronautica*, 2009, **65**, (3-4), pp 467-476.
6. KANDA, T., MASUYA, G. and WAKAMATSU, Y. Propellant feed system of a regeneratively cooled scramjet, *J Propulsion and Power*, 1991, **7**, (2), pp 299-301.
7. ROUDAKOV, A.S. and SEMENOV, V.L. Recent flight test results of the joint CIAM-NASA Mach 6.5 scramjet flight program, AIAA Paper 1998-164, 1998.
8. QIN, J., ZHOU, W., BAO, W. and YU, D. Thermodynamic analysis and parametric study of a closed Brayton cycle thermal management system for scramjet, *Int J Hydrogen Energy*, 2010, **35**, (1), pp 356–364.
9. SOBEL, D.R. and SPADACCINI, L.J. Hydrocarbon fuel cooling technologies for advanced propulsion, *J Engineering for Gas Turbines and Power*, 1997, **119**, pp 344–351.
10. BOUDREAU, A.H. Hypersonic air-breathing propulsion efforts in the Air Force Research Laboratory, AIAA Paper 2005-3255, 2005.
11. GASNER, J.A. and FUJIMURA, C. Evaluation of thermal management for a Mach 5.5 hypersonic vehicle, AIAA Paper 92-372, 1992.
12. QIN, J., BAO, W., ZHOU, W. and YU, D. Performance cycle analysis of an open cooling cycle for scramjet, *Proc. IMechE Part G: J Aerospace Engineering*, 2009, **223**, (6), pp 599-607.
13. BAO, W., QIN, J., ZHOU, W. and YU, D. Parametric performance analysis of multiple re-cooled cycle for hydrogen fueled scramjet, *Int J hydrogen energy*, 2009, **34**, (17), pp 7334–7341.
14. BAO, W., QIN, J., ZHOU, W. and YU, D. Performance limit analysis of recooled cycle for regenerative cooling systems, *Energy Conversion and Management*, 2009, **50**, (8), pp 1908-1914.
15. YOUN, B and MILLST, A.F. Cooling panel optimization for The active cooling system of a hHypersonic aircraft, *J Thermophysics and Heat Transfer*, 1995, **9**, (1), pp 136-143.
16. LEMMON, E.W., PESKIN, A.P. and FRIEND, D.G. NIST 12: Thermodynamic and Transport Properties of Pure Fluids. NIST Standard Reference Database Number 12, Version 5.0, National Institute of Standards and Technology, Boulder, CO, 2000.
17. SCHUFF, R., MAIER, M., SINDIY, O., ULRICH, C. and FUGGER, S. Integrated modelling and analysis for a LOX/Methane expander cycle engine: Focusing on regenerative cooling jacket design, AIAA Paper 2006-4534, July 2006.
18. TAYLOR, M.F. Correlation of local heat-transfer coefficients for single-phase turbulent flow of hydrogen in tubes with temperature ratios to 23, NASA TN D-4332, January 1968.
19. PEET, Y., SAGAUT, P. and CHARRON, Y. Pressure loss reduction in hydrogen pipelines by surface restructuring, *Int J Hydrogen Energy*, 2009, **34**, (21), pp 8964–8973.
20. DANIEL, K., PARRIS, D. and LANDRUM, B. Effect of tube geometry on regenerative cooling performance, AIAA Paper 2005-430, July 2005.
21. KANDA, T., MASUYA, G., WAKAMATSU, Y., CHINZEI, N. and KANMURI, A. Parametric study of airframe-Integrated scramjet cooling requirement, *J Propulsion and Power*, 1991, **7**, (3), pp 431-436.
22. LOCKE, J.M. and LANDRUM, D.B. Study of heat transfer correlations for supercritical hydrogen in regenerative cooling channels, *J Propulsion and Power*, 2008, **24**, (1), pp 94-103.
23. CENGEL Y.A. and BOLES M.A. *Thermodynamics*, 4th ed New York, US, McGraw-Hill, 2002.
24. BUCHMANN, O.A. *et al* Advanced fabrication techniques for hydrogen cooled engine structures, NASA CR 3949, November 1985.
25. DZIEDZIC, W.H., JONEST, S.C., GOULD, D.C. and PETLEY, D.H. Analytical comparison of convective heat transfer correlations in super-critical hydrogen, *J Thermophysics And Heat Transfer*, 1993, **7**, (1), pp 68-73.
26. SCOTTI. S.J., MARTIN, C.J. and LUCAS, S.H. Active cooling design for scramjet engines using optimization methods. 1988; NASA TM-100581.
27. WIETING, A.R. and GUY, R.W. Thermal-structural design/analysis of an airframe-integrated hydrogen-cooled scramjet, *J Aircr*, 1976, **13**, (3), pp 192-197.
28. BAO, W., QIN, J., ZHOU, W.X. and YU, D.R. Effect of cooling channel geometry on re-cooled cycle performance for hydrogen fueled scramjet, *Int J Hydrogen Energy*, 2010, **35**, (13), pp 7002–7011.
30. SORATO, S., PASCOVICI, D.S. and OGAJI, S.T. Investigating the emissions and performance of high bypass ratio aero-engines, *Proc IMechE Part G: J Aerospace Engineering*, 2008, **222**, (4), pp 463–471.
31. YANG J.C. and HUBER M.L. Analysis of thermodynamic processes involving hydrogen, *Int J Hydrogen Energy*, 2008, **33**, (16), pp 4413–4418.
32. BALTA, M.T., DINCER, I. and HEPBASLI, A. Thermodynamic assessment of geothermal energy use in hydrogen production, *Int J Hydrogen Energy*, 2009, **34**, (7), pp 2875–2880.
33. ROSSI, C.C.R.S., ALONSO, C.G. and ANTUNES, O.A.C. Thermodynamic analysis of steam reforming of ethanol and glycerine for hydrogen production, 2009, *Int J Hydrogen Energy*, **34**, (1), pp 323–332.
34. QIN, J., ZHOU, W., BAO, W. and YU, D. Thermodynamic optimization for a scramjet with Re-cooled Cycle, *Acta Astronautica*, 2010, **66**, (9-10), pp 1449-1457.
35. QIN, J., ZHOU, W., BAO, W. and YU, D. Irreversible cycle analysis of Re-Cooled Cycle for a Scramjet, *Proc IMechE Part G: J Aerospace Engineering*, 2009, **224**, (8), pp 912-926.
36. YANOVSKIY, L.S., BAYKOV, A.V. and MARTYNENKO, C.E. Cooling Character of hydrocarbon fuel in supercritical pressure, V nationwide aviation congress, Moscow, 2006 (In Russian).

https://doi.org/10.1017/S0001924000005479 Published online by Cambridge University Press